

CDMA-Based UHF-RFID System with Semi-Passive UHF Transponders

Andreas Loeffler, Ingo Altmann
 Chair of Information Technologies
 Friedrich-Alexander-University of Erlangen-Nuremberg
 Erlangen, Germany
 Email: {loeffler, altmann}@like.eei.uni-erlangen.de

Fabian Schuh
 Chair for Information Transmission
 Friedrich-Alexander-University of Erlangen-Nuremberg
 Erlangen, Germany
 Email: fabian.schuh@nt.eei.uni-erlangen.de

Abstract—RFID systems, in general, increase the efficiency of logistic systems, e.g., inventory of stocks. Unfortunately, present existing systems come fast to their limits if a certain number of RFID transponders must be *inventoried* in a limited period of time, as the channel access method of current RFID systems is based on Time Division Multiple Access. To shorten the inventory process, this work shows an implementation of an UHF RFID system based on semi-passive UHF transponders, using Code Division Multiple Access as anti-collision method. The work focuses on the uplink channel (tag to reader) that covers the transponders' backscattered signals. This channel access method enables simultaneous transfer of transponder data; i.e., all transponders in the field may respond at the same time within the same frequency band. The data transfer realized for the uplink channel uses a set of orthogonal spreading sequences (Gold codes) being different for every transponder. The RFID reader designed in this work despreads the backscattered signals and decodes the data of the different transponders. This work shows, in principle, the opportunity for a simultaneous data transfer on the uplink channel in RFID systems, which in turn may reduce the time needed for a complete inventory round. The entire system is build upon dedicated hardware, which is, also, a new aspect of this paper.

Keywords—Radio frequency identification; cdma; uhf; transponder; digital signal processors.

I. INTRODUCTION

Nowadays, the RFID technology makes it possible to register all purchased goods of a customer at a checkout counter, but so far it was not possible to accomplish an entire stock inventory within a big warehouse, at once. If several transponders are located within the reading range of a reader, it may come, with a certain probability, to overlapping signals (collisions) between some of these transponders. This is the reason why anti-collision procedures are widely used, which in turn provide methods trying to prevent transponders from broadcasting their information simultaneously. Existing RFID solutions, which are qualified to cope with reading several transponder in one *inventory round*, are based on Time Division Multiple Access (TDMA, see Figure 1a), meaning that the transponder in the reader's field transmit their data at different moments. Loeffler et al. show in [1] that code division multiple access (CDMA)-based systems (Figure 1b) may improve the process of inventory rounds.

Regarding TDMA-based systems, basically, one differ-

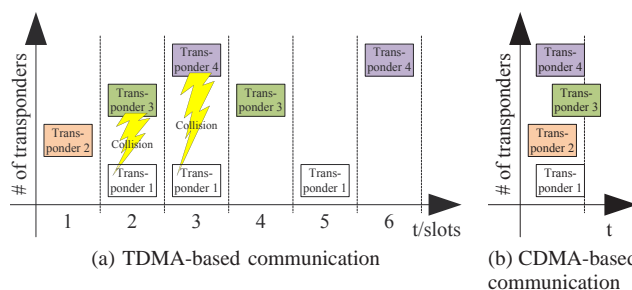


Figure 1. Different communication channel access techniques for RFID: TDMA, CDMA

entiates between the time-independent principle of pure or unslotted ALOHA and the temporally subdivided principle of slotted ALOHA. By using unslotted ALOHA, data is sent at the time it is available, therefore it is fairly unorganized. In contrast to unslotted ALOHA, the principle of slotted ALOHA defines the points of time a broadcasting of data is permitted. For instance, data transmitted by two transponders using slotted ALOHA only experience a collision if both transponders begin to send their data at the same time slot.

The anti-collision procedure of the EPC Gen2 standard [2], [3] is based on slotted ALOHA. A so called Q -parameter controls the overall inventory process. The choice of Q is a typical trade-off. Choosing a high Q will lead in fact to a smaller number of collisions but on the other hand to an increased time needed for an inventory round. A smaller Q will lead to less acquisition time, but to more collisions, indeed. In addition, the usage of TDMA methods brings the systems to its limits when a certain number of transponders have to be *inventoried* in a very short time. For instance, fast working production lines could face that kind of problem.

The introduction of Code Division Multiple Access may find a remedy ([1], [4]). The transponders, each equipped with a unique orthogonal spreading code, may send their data at any given point in time. Overlapping signals will be sorted out by the process of despreading.

The objective of this work is the realization of a CDMA-based RFID system using semi-passive UHF transponders, whereby the recognition of the transponders shall be done

quasi-simultaneously. This means that the transponders are transmitting data within the same time range and frequency band, in contrast to existing systems based on TDMA. For a first workaround this work concentrates on the uplink (i.e., tag to reader communication). The designed UHF transponders operate in semi-passive mode, meaning that the digital part of the transponders has an active power supply, whereas the radio frequency (RF) part works in passive mode (principle of backscatter [3]). The RFID reader, though, is separated into two parts. Part one, described as transmitting system, generates a sinusoidal wave at a certain UHF frequency. The frequency band for the usage of RFID within Europe is limited to a band between 865 MHz and 868 MHz. Part two, the receiving system, mixes down the backscattered signals, which are further processed analog, A/D converted and processed digital within a DSP. An overview of the complete system is given in Figure 3.

The paper is organized as follows. Following the introduction (Section I) and related work (Section II), Section III shows various anti-collision methods for RFID. This section focuses on ALOHA and slotted ALOHA as well as on some basic CDMA methods. Also, theoretical considerations are made to show the essential advantages of CDMA in RFID systems. Section IV goes into more detail regarding the combination of RFID and CDMA as channel access method. The proposed and realized CDMA-based RFID system is described in Section V. Within this section, the transmit stage, the transponder and the receiving stage are explained in detail. Section VI presents measurements regarding the system parts in the preceding section. Results are depicted in Section VII, whereas the article concludes with Section VIII.

II. RELATED WORK

There is still ongoing research in the topic of combining classic RFID and CDMA methods. Mazurek [5]–[7] describes an approach where active RFID transponders are used to implement a direct-sequence (DS) CDMA RFID uplink transmission. The overall system design is described in [5]. It consists of several tags working in the 433 MHz ISM (industrial, scientific and medical) radio band. 127+1 Gold chips are applied at a stated chip rate of the RFID tags with 97.75 kHz. As the RFID tags are active, the output power level of the tags' transmitters is -10 dBm. Also, this paper shows theoretical, simulated and experimental results of the implementation. More results of this system are shown in [6]. Mazurek presents in [7] a performance analysis of the proposed active RFID system with the unslotted DS-CDMA transmission scheme. According to his paper, the active RFID system with DS-CDMA is able to successfully read out three times more tags per kilohertz bandwidth (RFID uplink channel) than an ALOHA-based RFID system. This shows the available potential of CDMA in RFID systems.

Other work related to this subject mainly consists of theoretical work and carried out simulations. The work

done in [8] compares different approaches to overcome present limitations by simulating and evaluating slotted ALOHA, ID arbitration and direct-sequence CDMA. Lim and Mok [8] came to the result that the performance results of CDMA gives superior performance compared to the other two methods. Tseng and Lin [9] demonstrated (under usage of simulations) that the proposed Spreaded Partial-Q Slot Count algorithm outperforms existing anti-collision algorithms (such as common EPC Gen2) in terms of throughput. This algorithm is indeed a mixture of the commonly used EPC Gen2 anti-collision algorithm and a DS-CDMA approach.

A design of a CDMA-based transponder in HF-RFID (i.e., 13.56 MHz) is proposed by Fukumizu et al. [10]; the system is based on a PSK-like modulation scheme with a time hopping DS-CDMA multi-access, i.e., a combination of TDMA and CDMA. A SAW (surface acoustic wave) RFID tag is proposed in [11] and a prototype was tested at a frequency of 250 MHz.

The work from Rohatgi and Durgin [12] is in turn more closely related to this work. Nevertheless, basic differences are, e.g., the chosen chip rate, which is 1 kcps (chips per second), whereas this system operates with a minimum chip rate of 1.5 Mcps. Another difference is the underlying code sequence of the transponders. Rohatgi and Durgin [12] propose the usage of a PN-sequence (Pseudo Noise) in contrast to the Gold codes used in this work. The generation of orthogonal code sequences with different lengths is, e.g., described in [13] and will therefore not be part of this paper.

III. BASIC PRINCIPLES OF ANTI-COLLISION METHODS FOR RFID

This section shall outline some basic issues regarding anti-collision methods within RFID. Basic and state-of-the-art anti-collision methods are shown in Subsection III-A. Subsection III-B presents theoretical performance issues regarding the throughput by comparing state-of-the-art TDMA methods with CDMA anti-collision methods.

A. ALOHA and slotted ALOHA

Before elucidating the state-of-the-art anti-collision method for UHF RFID systems, the principle of ALOHA and unslotted ALOHA [14] is illustrated. The ALOHA protocol (or pure ALOHA), first published by Abramson [15], is a very simple transmission protocol. The transmitter sends its data, no matter if the transmission channel is free or not. This means the transmitter does not care about collisions with other transmitters. The transmitter resends its data later, if the acknowledgment from the receiver is missing. RFID systems based on the principle of pure ALOHA are, e.g., based on the TTF principle, i.e., transponder-talks-first. The IPX protocol from IPICO [16] is an example for RFID systems using unslotted or pure ALOHA.

The extended ALOHA protocol, called slotted ALOHA [17], introduces time slots in which the transmitter must send its data at the beginning. Therefore, collisions only occur within a full time slot. This extension doubles the maximum throughput of the system. Most current RFID protocols are based on the principle of slotted ALOHA, as is also the very common used EPC standard UHF Class-1 Generation-2 air interface protocol V1.2.0 (ISO 18000-6C), commonly known as “Gen2”. Basically, the “Gen2” standard works as follows. The standard defines, that every communication is triggered by the RFID reader, i.e., RTF (reader-talks-first). An inventory round, i.e., the process of detecting all available transponders, for instance, is started with the *Query*-command to acquire all transponders available in the read range. This command inherits a so called *Q*-parameter. Using this *Q*-parameter, every transponder generates a random number RN in the range $[0; 2^Q - 1]$ and initializes its internal slot counter with this random number. If, at a given moment, the value of the slot counter of one or more transponders equals 0, the transponders send a 16 bit random number called RN_{16} . After the acknowledgment of the RN_{16} through the reader, the electronic product code (EPC) is transmitted from the transponder to the reader and the transponder will be marked as *inventoried*. All the left-over (non-marked) transponders are prompted to decrement its slot counter by sending a *QueryRep*-command, and the procedure starts all over again. In the case of several transponders initializing their slot counters with the same random number RN , it will come sooner or later to a signal collision as the slot counters will reach zero at the same time slot. If the reader recognizes such a collision, another inventory round will be initiated to identify the left-over transponders. Therefore, a newly value of Q will be introduced and new random numbers will be calculated.

Lots of work has been done to improve the current EPC standard. Improving the current standard anti-collision method by choosing an appropriate value of Q , e.g., dynamically, is described in [18]–[20]. The right choice of Q is of great importance for the overall system performance, so that an accurate estimation would improve the time needed for an inventory round. Slightly new algorithms, based on the current EPC “Gen2” standard are outlined, e.g. in [21], [22]. New better performing algorithms for the slotted ALOHA protocol for RFID are described in [23]–[26]. A complete new system with time hopping on the communication link from tag to reader is outlined in [27].

B. Throughput in TDMA- and CDMA-based Systems

The throughput S in dependence of the traffic channel rate G describes the performance of a given transmission system regarding how many packets must be transmitted (statistically) until a successful transmission occurs. This

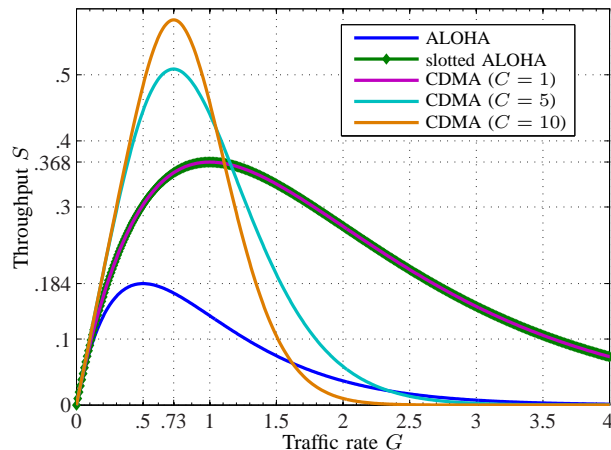


Figure 2. Various throughputs S over traffic rate G for ALOHA, slotted ALOHA and CDMA

statement is given with the term $\frac{G}{S}$ as described by Kleinrock and Tobagi [28]. The reciprocal of this term, i.e., $\frac{S}{G}$ defines accordingly the probability of a successful transmission. The channel capacity is determined by maximizing S with respect to G [28]. According to Abramson [15] the pure ALOHA transmission has a relation between S and G of

$$S = G e^{-G} \quad (1)$$

, whereas the throughput of the slotted ALOHA transmission is defined after Roberts [17] with

$$S = G e^{-2G} \quad (2)$$

. Accordingly, the maximum channel capacity is $\frac{1}{2e} \approx 18.4\%$ for pure ALOHA and $\frac{1}{e} \approx 36.8\%$ for slotted ALOHA.

For a fair comparison between CDMA-based systems and ALOHA systems, the total bandwidth has to be maintained the same for both systems. A CDMA system has a so called spreading factor C , which is proportional to the length of the spreading codes respectively the ratio between chip rate and bit rate (i.e., R_{chip}/R_{bit}) used. According to Linnartz and Vvedenskaya [29] the throughput S and the offered traffic rate G is

$$S = G e^{-CG} \sum_{k=0}^{C-1} \frac{(CG)^k}{k!} \quad (3)$$

. Setting $C = 1$ leads to the slotted ALOHA transmission scheme. Figure 2 shows various throughputs S over the traffic rate G . The figure shows the throughputs for ALOHA (channel capacity 18.4%), slotted ALOHA and CDMA with spreading factor $C = 1$ (channel capacity 36.8%), CDMA with $C = 5$ (channel capacity 50.87%) and CDMA with $C = 10$ (channel capacity 58.31%). This graph shows the basic difference between TDMA (ALOHA-based) and CDMA systems. In general, TDMA-based RFID

systems can handle much more RFID transponders with a lower overall throughput. CDMA-based system, on the other hand, are able to handle a limited amount of RFID tags with higher overall throughput. For instance, assuming a limited amount of RFID transponders for a traffic rate $G = 0.73$. The throughput of unslotted ALOHA would be $S_{\text{ALOHA}} = 16.95\%$ and the throughput of slotted ALOHA $S_{\text{unslotted ALOHA}} = 35.18\%$. A CDMA-based system with a spreading factor C of 10 would have there its maximum throughput of $S_{\text{CDMA}, C=10} = 58.31\%$. This scenario is shown in Figure 2.

Finally, it can be stated that CDMA-based RFID systems may be better for particular applications, in which the number of transponders is limited and the inventory process has to be made very fast, e.g., fast production lines and automation processes.

Particular slotted ALOHA CDMA systems and corresponding performances may be found in [30], [31]. Other works describe certain CDMA systems with error correction which really outperform the TDMA-based systems. Examples can be found in [32]–[36]. Also this list is not complete it gives a short overview of CDMA-based system performances.

IV. BASIC PRINCIPLES OF CDMA FOR RFID

This section shows some basic work regarding UHF RFID systems in conjunction with CDMA.

An IC design for an experimental transponder is offered in [37]. The transponder uses time-hopping DS-CDMA, but operates within the RFID HF region (13.56 MHz). Therefore, the transponder cannot be compared directly with the proposed approach, but shows, that a fully integrated circuit for future releases of CDMA-based RFID UHF transponders is possible. Wang et al. [38] describes an anti-collision method based on CDMA. Gold codes are used as spreading sequences. Also, a first design of a transponder is outlined. Within this design, a field effect transistor (FET) is used as source for backscattering. A new transmission scheme for TTF transponders is presented in [39]. The uplink is based on asynchronous DS-CDMA. It is shown, by simulation, that the proposed CDMA method outperforms the classical RFID transmission in terms of channel capacity. Also, Gold codes are used to separate the various RFID transponders.

Mutti and Floerkemeier [40] explore the chances how CDMA methods can help to inventory large buildups of transponders. A combination of slotted ALOHA and CDMA is proposed to receive better inventory results. Therefore, the CDMA method is only used at the moments when the channel collides. Also, they show that Gold codes are very suitable for the usage within RFID systems. Simulation results show that Gold codes outperform Kasami codes.

A new anti-collision method is presented in [9] with the goal to achieve a fast inventory process. A so called spread partial-Q slot count algorithm which is based on slotted

ALOHA CDMA increases the overall throughput at the cost of bandwidth and complexity.

Other algorithms are presented in [41], [42], where the throughput is increased by using dynamic slotted ALOHA CDMA algorithms with orthogonal variable spreading factors. Theoretic analysis and simulations show an increasing performance regarding the identification process. However, the proposed algorithms perform different, when the conditions of the RFID system changes. A better gain may only be achieved, if the system itself is involved into the design of the algorithms.

Another approach is described by Liu and Guo [4], that uses Huffman spreading sequences to improve the process of inventory. Therefore several performances have been compared. Simulation results show the increase in performance if proposed Huffman spreading sequences are used. Anyway, a direct hardware implementation has to consider the various states within the IQ constellation diagram to be imaged to the backscatterer modulator.

A minimum mean-squared error single user adaptive receiver for the asynchronous DS-CDMA system, based on the least-mean-square (LMS) algorithm is presented in [43]. The article states that the proposed algorithm achieves a faster convergence rate than the transversal LMS algorithm.

Wuu et al. [44] presents a zero-collision scheme, that is based on CDMA and hash-chain mechanisms. The results of the paper show that with the applied techniques, not only a zero-collision scheme, but also a secure channel may be realized to outperform standard technologies. Anyway, the authors assume, that CDMA can be implemented into RFID systems, particularly RFID transponders.

Summing up, it can be stated, that the usage of CDMA for RFID not only provides better system performance, but also offers advanced security issues. Furthermore, very low effort was put into the realization of such a CDMA-based RFID system as such. Therefore, this missing piece is one of the subjects of this work.

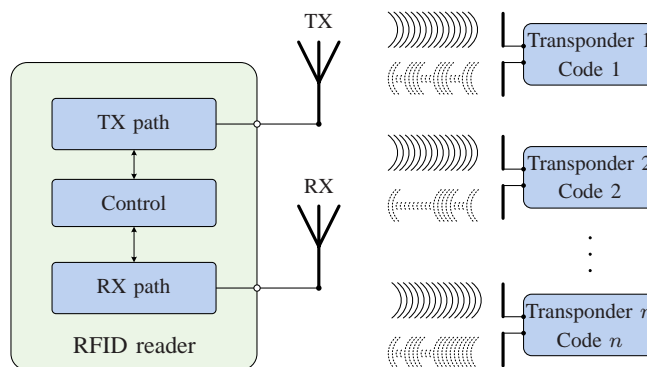


Figure 3. Basic architecture of RFID system

V. CDMA-BASED RFID SYSTEM

Within this section the basics of the proposed RFID system are presented. Going into more detail, subsection V-A shows the architecture of the *Transmitting System*, followed by subsection V-B presenting the proposed semi-passive RFID transponders and subsection V-C describing the *Receiving System*.

Figure 3 shows the basic architecture of the CDMA-based RFID system. Generally, it consists, as any other RFID system, too, of two major parts. First, the RFID reader itself and second, one or more transponders. The big difference between this system and other current systems is the channel access method in the uplink (transponder to reader communication) layer, in this case based on CDMA; this fact is illustrated in Figure 3 showing every transponder (Transponder 1 to Transponder n) with a unique spreading code (Code 1 to Code n).

The basic working principle is also indicated in Figure 3, showing the RFID reader with transmitting a sinusoidal wave over its transmit antenna TX, thus allowing the various transponders in the field to modulate and reflect (principle of backscatter) this incident wave back to the RFID reader. Therefore, the total backscattered signal consists of the additive superposition of n (if multipath is negligible) backscattered transponder signals with each transponder using its own unique spreading code. Receiving this superimposed signal over RX, the reader is, generally, able to separate the various transponder signals from each other (process of despreading) in order to restore the transponders' data.

Figure 3 and Figure 5, respectively, show the concept and the architecture of the realized RFID reader. The following paragraphs will refer to these figures.

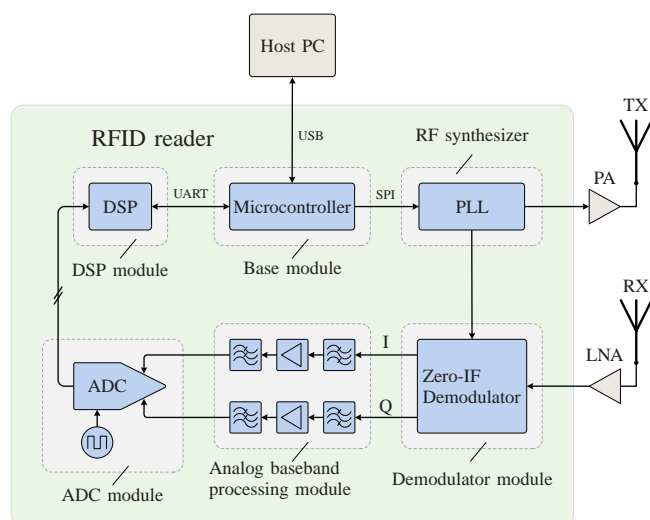


Figure 4. Basic concept of RFID reader

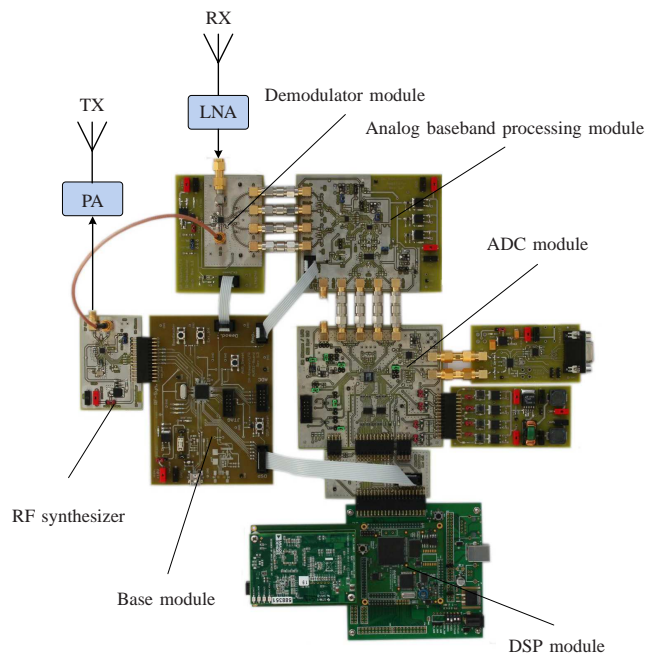


Figure 5. Architecture of CDMA-based RFID reader

A. Transmitting System

The proposed semi-passive UHF transponder works in accordance with the principle of backscattering. The incident wave to be backscattered is generated by the *Transmitting System*. Considering the RFID uplink channel (tag to reader), the introduced *Transmitting System* (see Figure 3 and Figure 5) consists of a PLL-based RF synthesizer (Figure 3 and Figure 5), generating a sine wave (here with $f_{\text{carrier}} = 866.5 \text{ MHz}$, maximum output power $P_{\text{out}} = 1 \text{ dBm}$ at 50Ω), an upstream power amplifier (PA, Gain $G_{PA} = 20 \text{ dB}$, 1 dB compression point = 24 dBm), and a linear polarized 50Ω antenna (TX, Gain $G_{TX} \approx 7 \text{ dBi}$). The purpose of the transmitter is to generate an RF wave to be reflected (backscattered) by the UHF transponder whereby the reflected wave is received by the *Receiving System* further discussed in subsection V-C.

It has to be mentioned that the RF synthesizer not only generates a sine wave for the transmitting part, but also for the receiving part of the system. Indeed, it is used as local oscillator (LO) source for the downmixing part of the receiver. However, both synthesized RF waves inherit the same frequency as they are both created by the same PLL; the waves only differ of π in phase.

B. Transponder

The major tasks of the semi-passive UHF transponders are:

- Generate spreading code
- Create spreaded data

- Modulate and reflect incoming RF signal at $f_{\text{carrier}} = 866.5 \text{ MHz}$ (principle of backscatter)

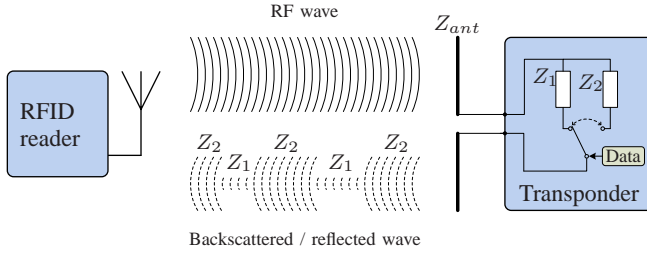


Figure 6. Basic function of RFID transponder

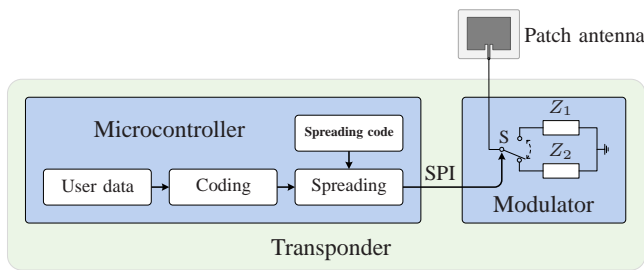


Figure 7. Concept of CDMA-based semi-passive UHF RFID transponder

Figure 6 shows the basic principle of an RFID transponder. An incident RF wave is reflected by the transponder. The phase and amplitude of the reflected wave is affected by three major issues: The first two issues are structural mode and antenna mode scattering [45], [46], the third issue is the multipath propagation. Multipath effects are a non-changeable fact, so they can be neglected at this point. The structural mode scattering of an antenna is dependent on the structure of the antenna itself (material, antenna geometry, etc.) and cannot be changed - therefore, the structural mode may not be used for a normal data transmission. The antenna mode scattering, on the other hand, describes the receiving and emitting effects of an antenna, which usually depend on the impedances used; particularly the impedance of the antenna Z_{ant} itself and the corresponding load impedance Z_{load} of the following transponder system. Assuming that Z_{load} can adopt two values being Z_1 and Z_2 . According to Figure 6 the antenna mode scattering may be changed by altering the load impedance Z_{load} of the transponder's antenna according to the data the transponder wants to send. Binary data may be send by altering Z_{load} between Z_1 and Z_2 , thus changing the reflection coefficient between Z_{ant} and Z_{load} , which in turn leads to an alteration of the reflection of the RF wave in phase and amplitude. Again, this only affects the antenna mode scattering. However, the total resulting backscattered signal is the superposition of the multipath signal, the structural mode scattering and antenna mode scattering effects. Measurements at the end of this

paper will show this effects.

Figure 7 shows the basic concept of the CDMA-based semi-passive transponder. A central microcontroller generates the binary output data stream (i.e., the already coded and spreaded user data) to drive the fast RF switch 'S', that alters between two impedance states Z_1 and Z_2 ; according to the binary state of the output data stream, a logical '1' triggers Z_2 , a logical '0' triggers Z_1 to be the corresponding load impedance. Therefore, the data stream directly affects the reflection coefficient. The performance of the uplink (tag to reader radio channel) depends very much on the modulation efficiency η_{mod} of the backscatter modulator [47]–[49], which basic calculation is subject of the following paragraph.

1) *Determining Load Impedances:* Assuming an antenna with complex antenna impedance

$$Z_{ant} = R_a + j X_a \quad (4)$$

with $R_a = R_r + R_l$ as the sum of radiation resistance R_r and real antenna losses R_l , and X_a as the imaginary part of the antenna impedance. The complex reflection coefficients $\Gamma_{1,2}$ between the antenna impedance and the load impedances $Z_{1,2}$ can be described as

$$\Gamma_{1,2} = \frac{Z_{1,2} - Z_{ant}^*}{Z_{1,2} + Z_{ant}} = \frac{Z_{1,2} - R_a + j X_a}{Z_{1,2} + R_a + j X_a} \quad (5)$$

According to Rembold [50] the modulation efficiency η_{mod} can be expressed as

$$\begin{aligned} \eta_{mod} &= \frac{P_{mod}}{P_{max}} = \frac{2}{\pi^2} |\Gamma_1 - \Gamma_2|^2 \\ &= \frac{2}{\pi^2} \left| \frac{Z_1 - R_a + j X_a}{Z_1 + R_a + j X_a} - \frac{Z_2 - R_a + j X_a}{Z_2 + R_a + j X_a} \right|^2 \\ &= \frac{8R_a^2}{\pi^2} \left| \frac{Z_1 - Z_2}{(Z_1 + R_a + j X_a)(Z_2 + R_a + j X_a)} \right|^2 \end{aligned} \quad (6)$$

, whereby P_{max} (the maximum receivable power of the antenna) and P_{mod} (the entire power with the information carrying signals) are defined as

$$P_{max} = \frac{1}{8} \frac{|U_0^2|}{R_a} = \frac{1}{2} |a|^2 \quad (7)$$

$$P_{mod} = \frac{|a|^2}{\pi^2} |\Gamma_1 - \Gamma_2|^2 \quad (8)$$

with U_0 as the antenna's open circuit voltage and a being the wave from the antenna impedance to the load impedance (see Rembold [50] for details).

Maximum modulation efficiency η_{mod} is achieved when the difference of the complex reflections coefficients Γ_1 and Γ_2 is maximum. Supposing two vectors (Γ_1 and Γ_2) in a complex coordinate system, the maximum difference between both vectors is achieved at the point when the phase φ_Γ differs with π under the assumption that the maximum

absolute value of any Γ is limited to 1. That determines the complex reflection coefficients $\Gamma_{1,2}$ to

$$\Gamma_1 = e^{j\varphi_{\Gamma,1}} \quad (9)$$

$$\Gamma_2 = e^{j\varphi_{\Gamma,1}+j\pi} \quad (10)$$

Setting $\varphi_{\Gamma,1}$ to 0 sets $\Gamma_{1,2}$ to ± 1 . According to Equation (5) this will define the load impedances to

$$Z_{1,2} = \frac{Z_{ant}^* + \Gamma_{1,2} Z_{ant}}{1 - \Gamma_{1,2}} \quad (11)$$

$$\rightarrow Z_1 = \frac{Z_{ant}^* + Z_{ant}}{0} = \pm\infty \quad (12)$$

$$\rightarrow Z_2 = \frac{Z_{ant}^* - Z_{ant}}{2} = \frac{-2jX_a}{2} = -jX_a \quad (13)$$

The antenna designed for the RFID transponders is a 50Ω patch antenna (Figure 9). Therefore the imaginary part (within the specified frequency range) $X_a \approx 0$. This determines $Z_2 = -jX_a \approx 0$. A load impedance of $Z_1 = \infty$ corresponds to an open circuit whereas $Z_2 = 0$ corresponds to a short circuit. Choosing open and short circuit states as desired load impedances, the maximum achievable modulation efficiency is, according to Equation (7), determined to be

$$\eta_{mod} = \frac{2}{\pi^2} |1 + 1|^2 = \frac{8}{\pi^2} \approx 81\% \quad (14)$$

. In order to have the maximum modulation efficiency for the CDMA-based RFID system, the load impedances of the realized semi-passive transponders are set to open and short circuit. By choosing these values as load impedances, one has to keep in mind, that this is only advisable for semi-passive UHF RFID transponders. If passive transponders are designed, one has to consider the power consumption into its calculations. Therefore, open and short circuit values are not suitable, as the backscattered power is, in fact, too high, as the transponder needs a large portion of the incoming power for supplying itself [51].

2) *Transponder Basics*: Figure 8 illustrates the concept of the transponder and Figure 9 shows one of the realized transponders to achieve the previously mentioned tasks. The microcontroller (μC) is powered by a power supply and may be user-controlled using USB or pushbuttons. The μC generates the unique spreading code and subsequently, the spreaded outgoing data. The data are forwarded to the SPI interface to drive the modulator of the transponder with different input voltages to adjust different load impedances respectively reflection coefficients of the modulator. The block diagram of the modulator (Figure 7) shows the principle of the proposed simple backscatter modulator. An example on how to design load modulators can be found in [52]. However, the incoming spreaded data stream is low-pass filtered to limit the outgoing bandwidth. As the modulator should be as simple as possible, an RF switch 'S' forms the interface between the logic data and the

backscattered HF wave. The inputs of the switch are driven by the spreaded data stream with two voltage levels (0 and 2.75 V) given by a buffer driver. One connection of the switch is linked to the patch antenna's microstrip line (50Ω); the ground connection is linked to the patch antenna's ground plane. By triggering the switch's input with the spreaded data to be sent, either Z_1 or Z_2 is connected to the antenna. This modification changes in turn the reflection of an incident electromagnetic wave. The difference of phase and amplitude of the reflection is a direct indicator for the efficiency of a backscattering modulator. As mentioned above the modulators load impedances are set to open and short circuit to achieve maximum modulation efficiency. An exemplary spectral extract of the backscattered output of the transponder, measured at the receiving antenna, is given in Figure 16. On closer inspection, one can see the spreaded data (chip rate is 1.5 Mcps) around the carrier frequency (866.5 MHz). As these data signal levels ($P \approx -90\text{ dBm} \pm 10\text{ dB}$) are not very high, an accurate implementation of the receiving system becomes necessary.

For a limited downlink (reader to tag) capability the transponders are equipped with a module for measuring the field strength (RSSI) and a module for measuring the frequency (RF Divider) of the incident RF wave emitted by the reader. The *RF Divider* is currently used to indicate the transponder to send its data as soon as a carrier between 865 MHz and 868 MHz is detected. The RSSI module is used for statistical measurements. Anyway, both modules are not part of this work.

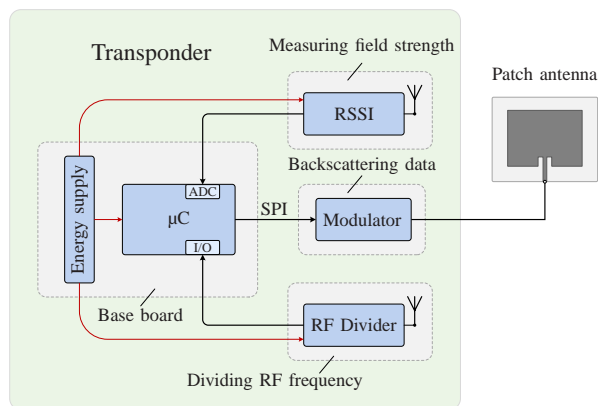


Figure 8. Block diagram of semi-passive UHF RFID transponder with limited downlink capabilities

3) *Modulator*: The transponder's modulator is one of the key components of the system. Usually, it effects the energy supply (only for passive working transponders) and the modulation efficiency (for passive and semi-passive working transponders) of transponders. Therefore, it has a direct effect for the maximum achievable range of such a system. The principle of the modulator has been already discussed above, so that this paragraph focuses primarily

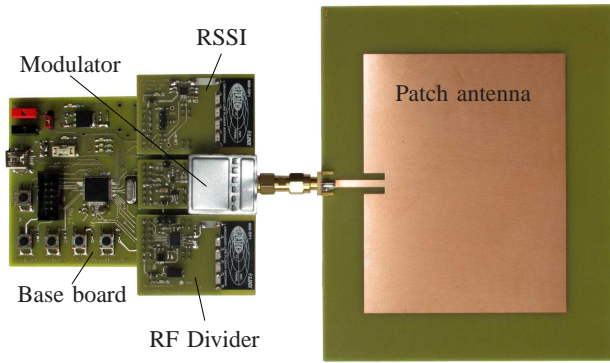


Figure 9. Prototype of semi-passive UHF RFID transponder

on the realization. Figure 10 shows the modulator, with and without RF shielding. The left part of the modulator is connected to the transponder's base board, the right SMA plug to the patch antenna as shown in Figure 9. The part within the RF shielding is responsible for the backscattering effects. A part of the incident RF wave is fed into the modulator. The part depends on the antenna (structural and antenna mode) and the reflection coefficient between antenna impedance Z_{ant} and the load impedance Z_{load} of the connected modulator. This part is fed into the RF switch and the load impedance (either Z_1 or Z_2), which corresponds to the current state of the switch. The state of the switch is defined by a buffered microcontroller output, which itself shows the current voltage of the binary data stream to be sent. In the case of Z_1 (open circuit state), the incident wave is entirely reflected with no phase shift. State Z_2 (short circuit) also corresponds to a total reflection, but with a phase shift of 180° .

Measuring the load impedances of the modulator show a very good accordance with the theoretical results. Figure 11 shows the reflection coefficients within a Smith chart. As one can see the phase difference is not exactly π . Z_2 (short circuit) has nearly short circuit properties; Z_2 (open circuit) has nearly open circuit properties. The frequency range of the measurement was between 852 MHz and 882 MHz.

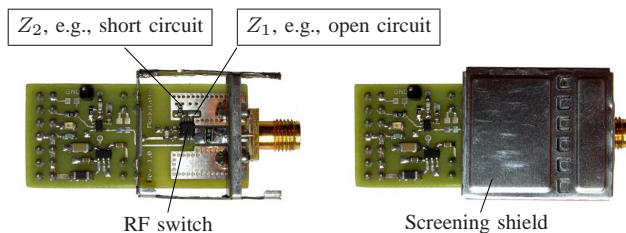


Figure 10. Backscatter modulator

4) *Gold Codes*: The choice of an appropriate set of spreading codes is a key issue when designing CDMA

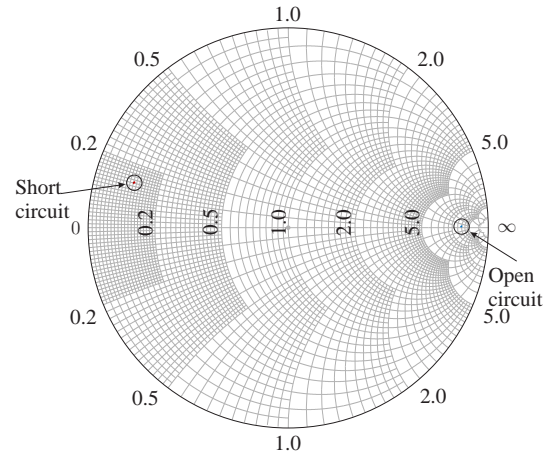
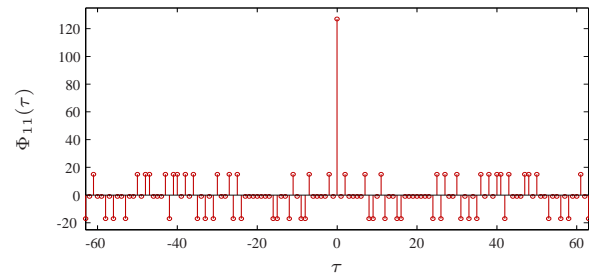
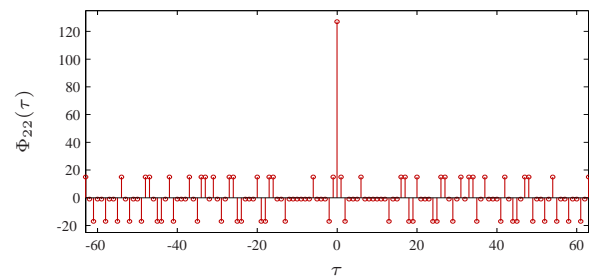


Figure 11. Smith chart of modulator



(a) ACF of Code 1



(b) ACF of Code 2

Figure 12. ACF of original Gold codes

systems. Gold codes seem to be one of the best codes to be used in UHF RFID systems. Mutti and Floerkemeier [40], for instance, state that Gold codes outperform Kasami codes. Moreover, one Gold code family contains a large number of unique codes, which provides a high probability of finding a well-suited set of codes for a system to be designed.

Gold codes, first introduced by Robert Gold [53], are commonly used in spread spectrum systems, such as WLAN and UMTS as well as in GPS (C/A code). The generation of Gold codes is quite simple as only two linear feedback shift registers (LFSR) are necessary to create one set of codes.

Other advantages of Gold code are:

- Good balance between auto- and cross-correlation
- Flexibility in code length
- No user synchronization necessary, i.e. the transponders need not to be synchronized among each other

Because of above mentioned advantages, the proposed CDMA-based system uses Gold sequences.

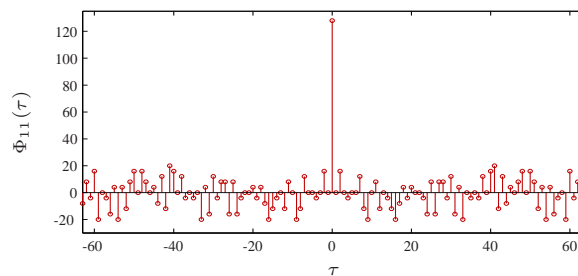
However, Gold codes have a length of $2^m - 1$ with m being the order of each linear feedback shift register. For reasons of flexibility a Gold code generator has been implemented on the transponder's 32 bit μC . The choice fell upon a Gold code length of 127 ($m = 7$). The characteristic polynomial is 137_{dec} for the first LFSR and 143_{dec} for the second one. The initial value for the first LFSR is 85_{dec} . By choosing two Gold codes (Code 1 and Code 2) the second LFSR is initialized with 127_{dec} for the first and with 111_{dec} for the second code. Then, a small adjustment was made to the generated Gold codes to be more compatible to the μC . A succeeding binary '0' is added to each code to move it to a length of 128 bit. To show the effect of this '0', the auto-correlation function (ACF) and cross-correlation function (CCF) have been evaluated for both Codes. Figure 12 shows the ACF Φ_{cc} of the original 127 bit Gold codes. Figure 13 illustrates the ACF $\Phi_{cc}(\tau)$ of the adjusted (127+1 bit) Gold codes. The results are slightly higher values beyond the peak value at $\tau = 0$. As not only the auto-correlation counts, the corresponding cross-correlation $\Phi_{12}(\tau)$ between the two codes are presented in Figure 14. As expected the values of the adjusted codes are slightly higher compared to the original ones, but without losing the typical noise-like character. This means, that the effect of the added '0' is negligible for further considerations. However, final system implementations have to consider that fact.

C. Receiving System

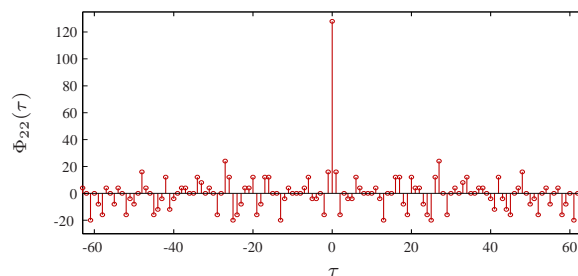
The major tasks of the *Receiving system* are:

- Receive incoming signals from several transponders, i.e., downmixing, analog baseband processing and A/D conversion
- Find separate data streams (transponders) by despread-ing, demodulating and decoding the signals

The *Receiving system* mainly consists of a hardware part that is needed to mix down the backscattered RF signal, centered at $f_c = 866.5 \text{ MHz}$, into baseband, despread, demodulate, and decode the baseband signal in order to determine the transponders' data. Figure 15 presents the structure of this receiving part of the RFID reader. The incoming RF signal is caught by a receiving antenna (RX) and amplified by a following low noise amplifier (LNA). A subsequent Zero-IF IQ-Demodulator mixes down the RF signal directly to baseband. The output of the demodulator consists of differential I- and Q-signals, which are band-pass filtered, twice

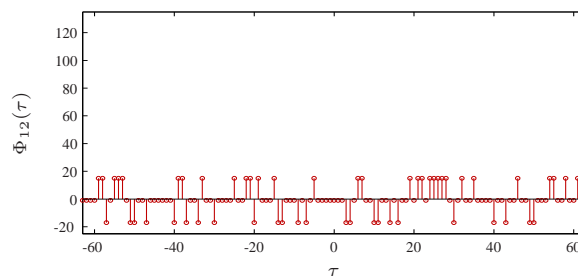


(a) ACF of Code 1

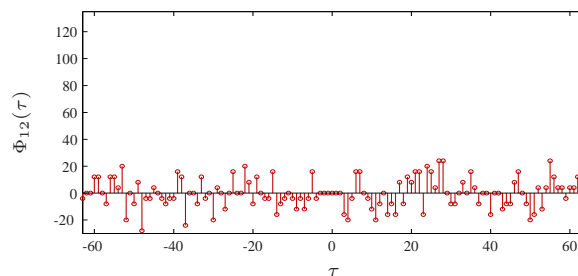


(b) ACF of Code 2

Figure 13. ACF of adjusted Gold codes



(a) CCF of original Code 1 and Code 2



(b) CCF of adjusted Code 1 and Code 2

Figure 14. CCF of both, original and adjusted Gold codes

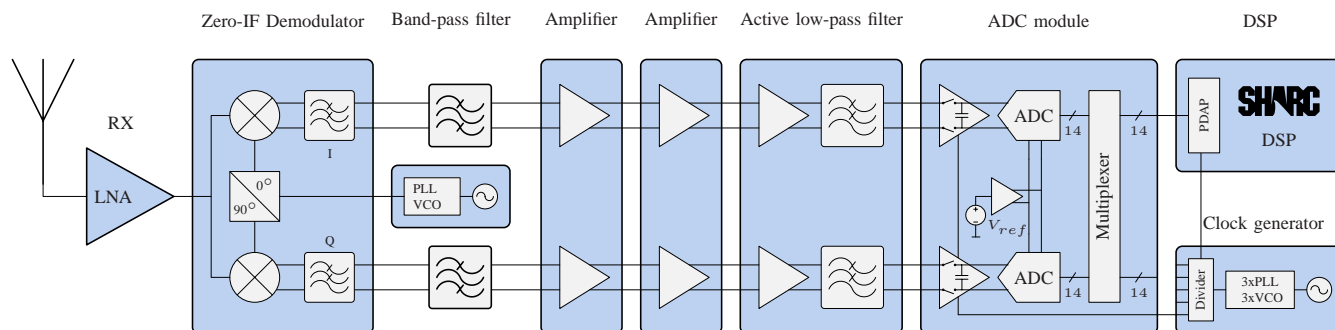


Figure 15. Architecture of receiving system

amplified and active low-pass filtered. It has to be mentioned that the IQ signals are completely handled differentially throughout the amplifier and filter stages to keep the signal-to-noise ratio (SNR) at a high level. The succeeding Analog-to-Digital conversion (ADC) module samples both, the I- and Q-signal, simultaneously. The A/D converted signals are fed into a digital signal processor (DSP) block with a data rate of 450 Mbps (Sampling of 2 channels with each channel having a resolution of 15 bit (14 data + 1 status bit) including a sampling rate of 15 Msps). The DSP module despreads, demodulates and decodes this data stream. The results are the user data of each recognized transponder.

The following paragraphs focus on the details of the receiving system.

1) *Demodulator*: The incoming low-noise amplified signal is fed into the demodulator. The demodulator uses the second RF synthesizer signal (the first is used as RF signal source for the transmit path, see above) as local oscillator (LO) source, to mix down the RF signal directly into baseband (Zero-IF). The demodulator is based on the LT5575 chip [54] from Linear Technology and 50 Ω -matched between 865 MHz and 868 MHz. The output of the demodulator is differential with 2 I- and 2 Q-signals, respectively.

2) *Band-Pass Filter*: The differential working band-pass filter, which succeeds the demodulator, is used to suppress the DC-part of the baseband signal, i.e. mainly the non-information carrying down-mixed carrier signal, and high-frequency disturbing signals (from the internal mixer of the demodulator). Therefore the passband is set between 16 kHz and 20 MHz.

3) *Amplifier Stage*: The following amplifier stage is built upon two differential amplifiers (LTC6421-20 [55] and LTC6420-20 [56]), each with a differential voltage gain of 10 V/V.

4) *Active Anti-Aliasing Filter*: The last analog signal processing stage is an active anti-aliasing filter for the succeeding ADC module. The cut-off frequency of the 4th order low-pass filter (Chebyshev characteristic) is currently set to 2.5 MHz. This stage is based on LT6604-2.5 [57] from

Linear Technology.

5) *A/D Conversion*: One very important part of the receiving system is a well-designed A/D conversion stage for the baseband signal. The subjective of the ADC module is a time synchron sampling of the differential I- and Q-signals. The module is based on a dual A/D converter of type AD9248 from Analog Devices [58]. Two channels may be sampled synchronously with a resolution of 14 bit per channel. Maximum sampling rate is 40 Msps. As the fast parallel input of the succeeding DSP module has only 20 bit the internal multiplexer of the A/D converter is used to transmit the I- and Q-data after each other. Therefore one status bit is used to indicate the current transmitted channel data. Here, the A/D converter is driven with 15 Msps per channel, which corresponds to an overall sampling clock rate of 30 MHz. The 14 bit per channel plus the status bit and the sampling rate, generate in total a data rate of 450 Mbps to be handled by the subsequent DSP module.

6) *DSP Module*: The purpose of the DSP is the handling of all calculations, necessary to evaluate the transponders' user data. Therefore, the following stages are necessary:

- Data acquisition (from ADC module)
- Despreading of baseband signals
- Demodulation of despread signals
- Decoding of demodulated data

The following paragraphs give a short introduction to these topics. The data acquisition phase has to be accomplished only once, against what the following stages have to be passed through by every transponder respectively spreading code available.

Data Acquisition: As the amount of data to handle is quite large (450 Mbps) the data streams are not handled in real time. However, through the usage of this DSP (ADSP-21469 from Analog Devices [59]) the processing speed is quite high. The A/D converted data signals are acquired through the DSP's PDAP (Parallel Data Acquisition Port) interface. From there, they are transferred to an internal 8x32 bit buffer. Finally, the data are passed via DMA access to an internal memory. As of limited memory capabilities the

data is transferred block-wise to the external memory. As the sampled values are stored as 32 bit values (DWORD), the amount of data for one shot (duration is $T_{shot} \approx 188 \mu\text{s}$) is 90112 samples per channel, so in total 720896 bytes or 704 kbytes.

Despreading: The process of despreading is the most calculation intensive operation the DSP has to handle. As this phase needs more time than the data acquisition process the system is, up-to-date not able to work real-time. Parallel processing would be a good solution. The DSP itself has a clock rate of 450 MHz.

Despreading data from the baseband signal has to be done for I- and Q-channel separately. The despreading operation is realized using the cross-correlation between I and Q signals and the origin codes used by every transponder in the field. If $s[k]$ is the I or Q signal and $c[k]$ one of the corresponding codes of one of the transponders, the cross-correlation $\Phi_{s,c}(\tau)$ between these signals is done by multiplying every time instance signal s with code c . Equation (15) shows the corresponding relationship between $c[k]$ and $s[k]$

$$[s \star c][\tau] = \Phi_{s,c}(\tau) = \sum_{t=-\infty}^{+\infty} s^*[t] \cdot c[\tau + t] \quad (15)$$

A code length of 128 chips corresponds to 1280 samples ($R_{chip} = 1.5 \text{ Msps}$ and $R_{sample} = 15 \text{ Msps}$) and 90112 samples per channel for I and Q. This results into 230,686,720 multiplications and 180,224 additions.

One goal was to reduce this high amount of operations. This is realized through estimation of the time moments the chips appear within the IQ signals. This estimation method works as follows. The IQ baseband signal is sampled and correlated among the first $2 \cdot 1280 = 2560$ samples. This results in 6,553,600 multiplications and 5120 additions. The first maximum, corresponding to the first peak indicates the initial index i_0 to start the despreading process. The following peaks are estimated by jumping from i_0 , 1280 samples ahead. As certain incertitudes (oscillators, etc.) will lead to synchronization errors, the correlation is not only made at sample index $i_0 + n \cdot 1280$, but at 5 samples before and after the estimated time index. That means, the second peak is determined by executing the cross-correlation $\Phi_{i,1}(\tau)$ as given in Equation (16).

$$\Phi_{i,1}(\tau) = \sum_{t=i_0+1280-5}^{i_0+1280+5} s^*[t] \cdot c[\tau + t] \quad (16)$$

The result is 11 correlations per peak and a new synchronization index, as the new peak indicates the next starting point for the succeeding peak estimation. With 70 data peaks within one shot and 1 within the initial guess, the total number of correlations per channel is $2560 + 69 \cdot 11 = 3319$. This leads to 8,496,640 multiplications and 6,638 additions

in total for both channels. This is only 3.6% of the full correlation.

Demodulation: The process of demodulation inherits the merge of the I and Q signals. According to their signal quality, estimated through the maximum correlation values, the signals are weighted and superimposed. This process of demodulation is beyond this paper's scope and not further described.

Decoding User Data: The demodulated signal stream is Manchester coded [1] and needs to be decoded accordingly. The resulting data stream corresponds to the transponder's respectively the user data.

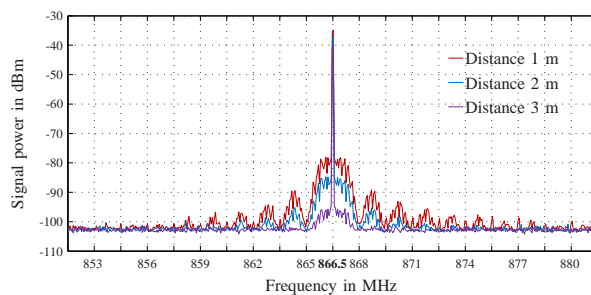


Figure 16. Spectrum of backscattered signal from transponder

VI. MEASUREMENTS

This section presents measurements of various parts of the system, including transponder, analog baseband processing and DSP.

A. Transponder Measurements

Figure 16 shows the spectrum of the backscattered transponder signals. For this measurement an RF signal ($P_{TX} = 10 \text{ dBm}$, $f_{carrier} = 866.5 \text{ MHz}$) is fed into the linear polarized transmit antenna. One transponder is placed at a distance of 1, 2 and 3 m. The resulting reflected signal spectrum after the receiving antenna is shown in Figure 16. As expected, the backscattered signal parts drop with increasing distance from the reader's antennas.

The IQ constellation diagrams of the received RF signal are shown throughout Figure 17 to Figure 19. It can be shown that the backscattered signals show a mixture between ASK and PSK modulation. For instance, as in Figure 17, the mean of the data points (from the two states of the one transponder) is not the origin (0,0). This discrepancy is the effect of multipath and structural antenna mode scattering. Same applies for Figure 18 with 2 transponders, generating $2^2 = 4$ constellation points, and Figure 19 with 3 transponders, generating $2^3 = 8$ constellation points. The number of constellation points for n transponders is 2^n because all n transponders have 2 states sharing the same coherent RF signal from the reader.

However, as expected the transponders show a near exact

BPSK modulation (as configured in subsection V-B3), if the ASK part is neglected.

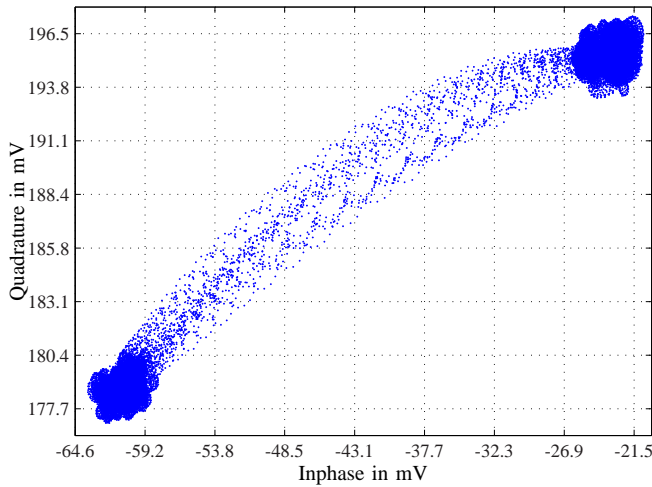


Figure 17. IQ constellation diagram for 1 transponder

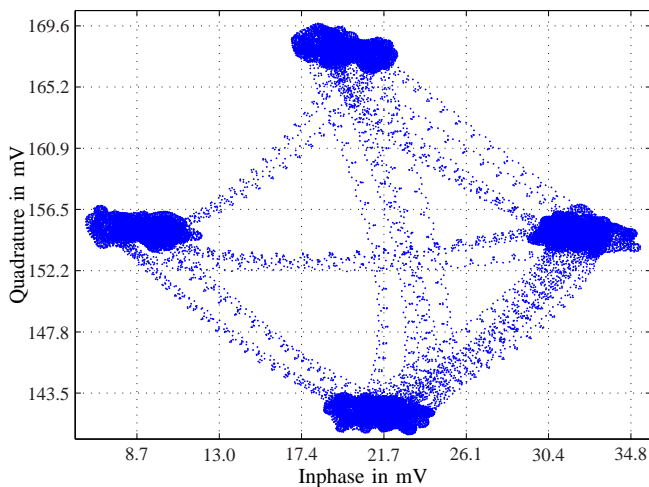


Figure 18. IQ constellation diagram for 2 transponders

B. RX Measurements

Two measurements have been carried out to show the basic working principle of the analog baseband processing module. The goal of this module is the signal conditioning for the succeeding ADC module. Figure 20 shows the output of the demodulator, i.e. the I- and Q-signals. As mentioned above these signals are handled differentially (I_+ , I_- , Q_+ and Q_-). To simplify matters the differential signals have been put together ($I = I_+ - I_-$ and $Q = Q_+ - Q_-$). The signals are amplified and filtered with a resulting signal as shown in Figure 21. The signals were recorded with 2 transponders in the field. As in the IQ measurements before, 2 transponders generate $2^2 = 4$ different signal levels (evaluated from Figure 21):

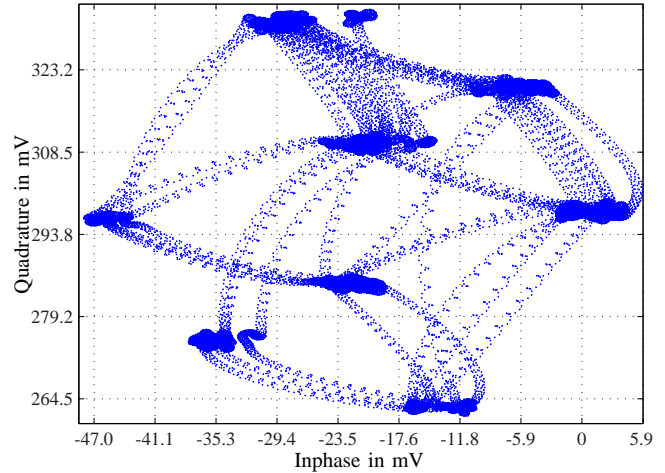


Figure 19. IQ constellation diagram for 3 transponders

- 1) $0.1 \text{ V} + j0.2 \text{ V}$
- 2) $0.3 \text{ V} - j0.4 \text{ V}$
- 3) $-0.2 \text{ V} - j0.2 \text{ V}$
- 4) $-0.4 \text{ V} + j0.5 \text{ V}$

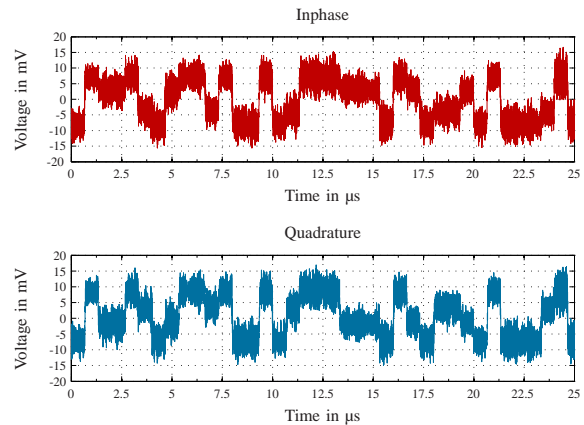


Figure 20. IQ signal after demodulator / 2 Transponders

C. DSP Measurements

The DSP module comes with some debugging functionalities. One of these functionalities is able to provide the DSP values, from its internal or external memories, via USB to a host PC. Figure 22 shows the results of a full cross-correlation. For simplicity the CCFs have been normalized to one. The values show the maximum number of samples (90112) and the peaks, with each peak describing a bit. The value of the bit may be positive (+1) or negative (-1). The difference between the peaks and the noise floor is an indicator for the quality of the communication link.

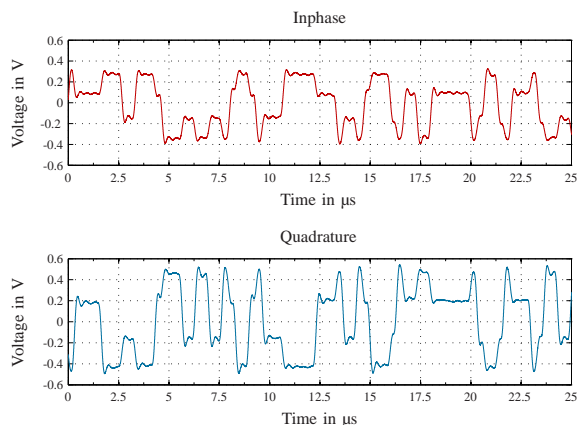


Figure 21. IQ signal after baseband processing / 2 Transponders

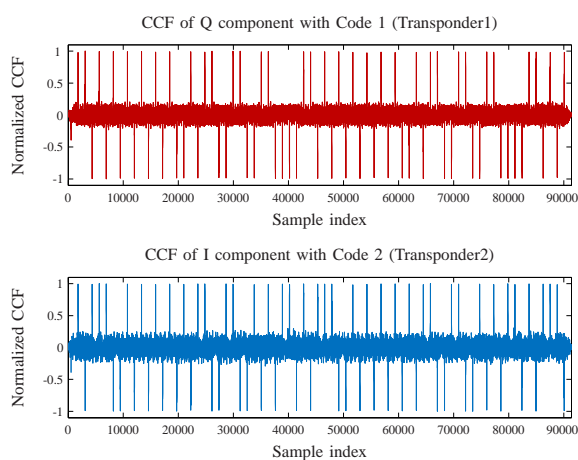


Figure 22. Cross-correlation of signals with origin spreading codes - Process of despreading / 2 Transponders

VII. RESULTS

According to the measurements the proposed system worked as expected. It was proved that the UHF RFID system for broadcasting information data using a CDMA method worked out very good. During the experiments there was a maximum distance to the antennas being around 15 m. The transmitted RF-power at 866.5 MHz was 20 dBm. The introduced transponders are semi-passive, which means that the communication link is still passive, whereas the data generation (on the transponder's side) is active, driven by 3.3 V power supplies.

Smaller problems arose, when various transponder had a different path length to the antennas. In that case one transponder (the nearest) dominated the second transponder (more far away) which often occurred to a non-detection of transponder two. This problem is known in CDMA systems and is referred to as near-far problem [60]. One possibility to reduce the near-far effect is the usage of Huffman sequences [4]. But this approach asks for more than 2 states of the load

impedance of the transponder's modulator. Nevertheless, carried out indoor experiments showed that the near-far effect of the proposed system is, in fact, very low.

Also, theoretical work, which states an advantage of CDMA-based RFID systems compared to state-of-the-art RFID systems based on TDMA methods, complies with the measured results of the proposed CDMA-based UHF RFID system.

VIII. CONCLUSION

This article presented a realization of a CDMA-based RFID system working in the UHF region. The system itself is build upon a *Transmitting system* providing a continuous electromagnetic wave. This emitted RF carrier is backscattered through one or more designed UHF tags. Each of these semi-passive operating transponders generate a unique spreading sequence. The proposed spreading sequences are Gold codes providing a good orthogonality. A simple modulator on the transponder generates the desired backscatter signal. The *Receiving system* captures this signal by down mixing the RF signal to baseband. Further analog signal processing and subsequent A/D conversion gives the DSP the chance to despread, demodulate and decode the desired transponder signals.

The significant advantage of such a structure compared to present systems lies in the ability to avoid particular TDMA-based anti-collision schemes. This, indeed, will lead to less time needed for *inventorizing* RFID tags, as this can be achieved within one time slot. Topics for future research are, regarding the receiver side, the need for much more computational resources (RAKE receiver, [61]) and the near-far problem, CDMA-based systems have to deal with.

REFERENCES

- [1] A. Loeffler, F. Schuh, and H. Gerhaeuser, "Realization of a CDMA-based RFID System Using a Semi-active UHF Transponder," in *Wireless and Mobile Communications (ICWMC), 2010 6th International Conference on*, Sep. 2010, pp. 5–10.
- [2] *Class 1 Generation 2 UHF Air Interface Protocol Standard "Gen 2"*, EPCglobal Inc. Std. UHF Class 1 Gen 2 Standard v. 1.2.0, 2008.
- [3] K. Finkeneller, *RFID handbook*. Wiley West Sussex, England, 2003.
- [4] H. Liu and X. Guo, "A passive UHF RFID system with Huffman sequence spreading backscatter signals," in *Proceedings of the 1st international conference on The internet of things*. Springer-Verlag, 2008, pp. 184–195.
- [5] G. Mazurek, "Design of RFID system with DS-CDMA transmission," in *Automation Science and Engineering, 2008. CASE 2008. IEEE International Conference on*, Aug. 2008, pp. 703–708.

- [6] —, “Experimental RFID system with active tags,” in *Signals and Electronic Systems, 2008. ICSES '08. International Conference on*, Sep. 2008, pp. 507–510.
- [7] —, “Active RFID System With Spread-Spectrum Transmission,” *Automation Science and Engineering, IEEE Transactions on*, vol. 6, no. 1, pp. 25–32, Jan. 2009.
- [8] A. Lim and K. Mok, “A study on the design of large-scale mobile recording and tracking systems,” in *System Sciences, 1998., Proceedings of the Thirty-First Hawaii International Conference on*, vol. 7, Jan 1998, pp. 701–710 vol.7.
- [9] D.-F. Tseng and Z.-C. Lin, “An Anti-Collision Algorithm in RFID Systems Based on Interference Cancellation and Tag Set Partitioning,” in *Vehicular Technology Conference, 2008. VTC Spring 2008. IEEE*, May 2008, pp. 1609–1614.
- [10] Y. Fukumizu, M. Nagata, S. Ohno, and K. Taki, “A Design of Transponder IC for Highly Collision Resistive RFID Systems,” in *Advanced System Integrated Circuits 2004. Proceedings of 2004 IEEE Asia-Pacific Conference on*, Aug. 2004, pp. 438–439.
- [11] J. Pavlina, B. Santos, N. Kozlovski, and D. Malocha, “SAW wireless, passive sensor spread spectrum platforms,” in *Ultrasonics Symposium, 2008. IUS 2008. IEEE*, Nov. 2008, pp. 1112–1115.
- [12] A. Rohatgi and G. Durgin, “Implementation of an Anti-Collision Differential-Offset Spread Spectrum RFID System,” in *IEEE Antennas and Propagation Society International Symposium 2006*, 2006, pp. 3501–3504.
- [13] A. Hottinen and K. Pehkonen, “A flexible multirate cdma concept with multiuser detection,” in *Spread Spectrum Techniques and Applications Proceedings, 1996., IEEE 4th International Symposium on*, vol. 2, Sep 1996, pp. 556–560 vol.2.
- [14] D. Bertsekas and R. Gallager, *Data networks (2nd ed.)*. Upper Saddle River, NJ, USA: Prentice-Hall, Inc., 1992.
- [15] N. Abramson, “THE ALOHA SYSTEM: another alternative for computer communications,” in *Proceedings of the November 17-19, 1970, fall joint computer conference*, ser. AFIPS '70 (Fall). New York, NY, USA: ACM, 1970, pp. 281–285. [Online]. Available: <http://doi.acm.org/10.1145/1478462.1478502>
- [16] IPICO, “IPICO’s IP-X RFID Air-interface Protocol,” Mar. 2009. [Online]. Available: <http://www.ipico.com/>
- [17] L. G. Roberts, “ALOHA packet system with and without slots and capture,” *SIGCOMM Comput. Commun. Rev.*, vol. 5, pp. 28–42, April 1975. [Online]. Available: <http://doi.acm.org/10.1145/1024916.1024920>
- [18] L.-C. Wang and H.-C. Liu, “A Novel Anti-Collision Algorithm for EPC Gen2 RFID Systems,” in *Wireless Communication Systems, 2006. ISWCS '06. 3rd International Symposium on*, Sep. 2006, pp. 761–765.
- [19] Y. Maguire and R. Pappu, “An Optimal Q-Algorithm for the ISO 18000-6C RFID Protocol,” *Automation Science and Engineering, IEEE Transactions on*, vol. 6, no. 1, pp. 16–24, Jan. 2009.
- [20] P. Pupunwiwat and B. Stantic, “A RFID Explicit Tag Estimation Scheme for Dynamic Framed-Slot ALOHA Anti-Collision,” in *Wireless Communications Networking and Mobile Computing (WiCOM), 2010 6th International Conference on*, Sep. 2010, pp. 1–4.
- [21] D. Lee, O. Bang, S. Im, and H. Lee, “Efficient dual bias Q-Algorithm and optimum weights for EPC Class 1 Generation 2 Protocol,” in *Wireless Conference, 2008. EW 2008. 14th European*, Jun. 2008, pp. 1–5.
- [22] Y. Cui and Y. Zhao, “A modified Q-parameter anti-collision scheme for RFID systems,” in *Ultra Modern Telecommunications Workshops, 2009. ICUMT '09. International Conference on*, Oct. 2009, pp. 1–4.
- [23] J. H. Choi, D. Lee, and H. Lee, “Query tree-based reservation for efficient RFID tag anti-collision,” *Communications Letters, IEEE*, vol. 11, no. 1, pp. 85–87, Jan. 2007.
- [24] O. Bang, S. Kim, and H. Lee, “Identification of RFID tags in dynamic framed slotted Aloha,” in *Advanced Communication Technology, 2009. ICACT 2009. 11th International Conference on*, vol. 01, Feb. 2009, pp. 354–357.
- [25] D. Liu, Z. Wang, J. Tan, H. Min, and J. Wang, “ALOHA algorithm considering the slot duration difference in RFID system,” in *RFID, 2009 IEEE International Conference on*, Apr. 2009, pp. 56–63.
- [26] S. Makwimanloy, P. Kovintavewat, U. Ketprom, and C. Tantibundhit, “A novel anti-collision algorithm for high-density RFID tags,” in *Electrical Engineering/Electronics, Computer, Telecommunications and Information Technology, 2009. ECTI-CON 2009. 6th International Conference on*, vol. 02, May 2009, pp. 848–851.
- [27] Z. Zhang, Z. Lu, Z. Pang, X. Yan, Q. Chen, and L.-R. Zheng, “A Low Delay Multiple Reader Passive RFID System Using Orthogonal TH-PPM IR-UWB,” in *Computer Communications and Networks (ICCCN), 2010 Proceedings of 19th International Conference on*, Aug. 2010, pp. 1–6.
- [28] L. Kleinrock and F. Tobagi, “Packet Switching in Radio Channels: Part I—Carrier Sense Multiple-Access Modes and Their Throughput-Delay Characteristics,” *Communications, IEEE Transactions on*, vol. 23, no. 12, pp. 1400–1416, Dec. 1975.
- [29] J.-P. M. Linnartz and N. D. Vvedenskaya, “DS-CDMA Packet Network with Random Access,” Dec. 2010. [Online]. Available: <http://www.wirelesscommunication.nl/reference/chaptr06/stack/cdmastck.htm>
- [30] S. Gopalan, G. Karystinos, and D. Pados, “Capacity, throughput, and delay of slotted ALOHA DS-CDMA links with adaptive space-time auxiliary-vector receivers,” *Wireless Communications, IEEE Transactions on*, vol. 4, no. 1, pp. 79–92, Jan. 2005.
- [31] A. Sakata, T. Yamazato, H. Okada, and M. KATAYAMAT, “Throughput Comparison of CSMA and CDMA slotted ALOHA in Inter-Vehicle Communication,” in *Telecommunications, 2007. ITST '07. 7th International Conference on ITS*, Jun. 2007, pp. 1–6.

- [32] A. Sastry, "Effect of Acknowledgment Traffic on the Performance of Slotted ALOHA-Code Division Multiple Access Systems," *Communications, IEEE Transactions on*, vol. 32, no. 11, pp. 1219 – 1222, Nov. 1984.
- [33] Z. Liu and M. El Zarki, "Performance analysis of DS-CDMA with slotted ALOHA random access for packet PCNs," in *Personal, Indoor and Mobile Radio Communications, 1994. Wireless Networks - Catching the Mobile Future., 5th IEEE International Symposium on*, vol. 4, Sep. 1994, pp. 1034 – 1039 vol.4.
- [34] R. van Nee, R. van Wolfswinkel, and R. Prasad, "Slotted ALOHA and code division multiple access techniques for land-mobile satellite personal communications," *Selected Areas in Communications, IEEE Journal on*, vol. 13, no. 2, pp. 382 –388, Feb. 1995.
- [35] F. L. Lo, T. S. Ng, and T. Yuk, "Performance analysis of a fully-connected, full-duplex CDMA ALOHA network with channel sensing and collision detection," *Selected Areas in Communications, IEEE Journal on*, vol. 14, no. 9, pp. 1708 –1716, Dec. 1996.
- [36] Q. Liu, E.-H. Yang, and Z. Zhang, "Throughput analysis of CDMA systems using multiuser receivers," *Communications, IEEE Transactions on*, vol. 49, no. 7, pp. 1192 –1202, Jul. 2001.
- [37] Y. Fukumizu, M. Nagata, S. Ohno, and K. Taki, "A design of transponder IC for highly collision resistive RFID systems," in *Advanced System Integrated Circuits 2004. Proceedings of 2004 IEEE Asia-Pacific Conference on*, Aug. 2004, pp. 438 – 439.
- [38] P. Wang, A. Hu, and W. Pei, "The Design of Anti-collision Mechanism of UHF RFID System based on CDMA," in *Circuits and Systems, 2006. APCCAS 2006. IEEE Asia Pacific Conference on*, Dec. 2006, pp. 1703 –1708.
- [39] G. Mazurek, "Collision-Resistant Transmission Scheme for Active RFID Systems," in *EUROCON, 2007. The International Conference on Computer as a Tool*, Sep. 2007, pp. 2517 –2520.
- [40] C. Mutti and C. Floerkemeier, "CDMA-based RFID Systems in Dense Scenarios: Concepts and Challenges," in *RFID, 2008 IEEE International Conference on*, Apr. 2008, pp. 215–222.
- [41] D. Yang, Y. Chen, and B. Wang, "RFID anti-collision algorithm in logistics service system," in *Service Operations and Logistics, and Informatics, 2008. IEEE/SOLI 2008. IEEE International Conference on*, vol. 2, Oct. 2008, pp. 1891 – 1896.
- [42] W. Bisheng, Y. Dongkai, and Z. Qishan, "Efficient Identification UHF RFID system scheme based on combination of DFSA and OVSF-CDMA," *IEICE Electronics Express*, vol. 5, no. 22, pp. 954–961, 2008.
- [43] C. Paleologu, C. Vlădeanu, and S. El Assad, "Fast Convergence Least-Mean-Square Algorithms for MMSE Receivers in DS-CDMA Systems," *International Journal On Advances in Networks and Services*, vol. 1, no. 1, 2008.
- [44] L.-C. Wu, Y.-J. Chen, C.-H. Hung, and W.-C. Kuo, "Zero-Collision RFID Tags Identification Based on CDMA," in *Information Assurance and Security, 2009. IAS '09. Fifth International Conference on*, vol. 1, Aug. 2009, pp. 513 – 516.
- [45] R. Hansen, "Relationships between antennas as scatterers and as radiators," *Proceedings of the IEEE*, vol. 77, no. 5, pp. 659 –662, May 1989.
- [46] K. Penttila, M. Keskilammi, L. Sydanheimo, and M. Kivikoski, "Radar cross-section analysis for passive RFID systems," *Microwaves, Antennas and Propagation, IEE Proceedings -*, vol. 153, no. 1, pp. 103 – 109, Feb. 2006.
- [47] U. Karthaus and M. Fischer, "Fully integrated passive UHF RFID transponder IC with 16,7 μ W minimum RF input power," *IEEE*, vol. 38, no. 10, pp. 1602–1608, 2003.
- [48] F. Fuschini, C. Piersanti, F. Paolazzi, and G. Falciasecca, "On the Efficiency of Load Modulation in RFID Systems Operating in Real Environment," *Antennas and Wireless Propagation Letters, IEEE*, vol. 7, pp. 243 –246, Mar. 2008.
- [49] P. Nikitin and K. Rao, "Antennas and propagation in uhf rfid systems," in *RFID, 2008 IEEE International Conference on*, Apr. 2008, pp. 277 –288.
- [50] B. Rembold, "Optimum modulation efficiency and sideband backscatter power response of RFID-tags," *Frequenz - Journal of RF-Engineering and Telecommunications*, vol. 63, no. 1 -2, pp. 9 –13, Jan. 2009.
- [51] D. Dobkin, *The RF in RFID: passive UHF RFID in practice*. Newnes, 2008.
- [52] D. Pardo, A. Vaz, S. Gil, J. Gomez, A. Ubarretxena, D. Puente, R. Morales-Ramos, A. Garcia-Alonso, and R. Berenguer, "Design criteria for full passive long range uhf rfid sensor for human body temperature monitoring," in *RFID, 2007. IEEE International Conference on*, March 2007, pp. 141–148.
- [53] R. Gold, "Optimal binary sequences for spread spectrum multiplexing (Corresp.)," *Information Theory, IEEE Transactions on*, vol. 13, no. 4, pp. 619 – 621, Oct. 1967.
- [54] Linear Technology, "LT5575 - 800MHz to 2.7GHz High Linearity Direct Conversion Quadrature Demodulator," Oct. 2010. [Online]. Available: <http://www.linear.com/pc/productDetail.jsp?navId=H0,C1,C1011,C1725,P36240>
- [55] —, "LTC6421-20 - Dual Matched 1.3GHz Differential Amplifiers/ADC Drivers," Oct. 2010. [Online]. Available: <http://www.linear.com/pc/productDetail.jsp?navId=H0,C1,C1154,C1009,C1126,P80589>
- [56] —, "LTC6420-20 - Dual Matched 1.8GHz Differential Amplifiers/ADC Drivers," Oct. 2010. [Online]. Available: <http://www.linear.com/pc/productDetail.jsp?navId=H0,C1,C1154,C1009,C1126,P80614>
- [57] —, "LT6604-2.5 - Dual Very Low Noise, Differential Amplifier and 2.5MHz Lowpass Filter," Oct. 2010. [Online]. Available: <http://www.linear.com/pc/productDetail.jsp?navId=H0,C1,C1154,C1008,C1148,P85251>

- [58] Analog Devices, “AD9248: Dual 14-Bit, 20/40/65 MSPS, 3 V Analog-to-Digital Converter,” Oct. 2010. [Online]. Available: <http://www.analog.com/en/analog-to-digital-converters/ad-converters/ad9248/products/product.html>
- [59] —, “ADSP-21469: High Performance Fourth Generation DSP,” Oct. 2010. [Online]. Available: <http://www.analog.com/en/embedded-processing-dsp/sharc/adsp-21469/processors/product.html>
- [60] J. Andrews, “Interference cancellation for cellular systems: A contemporary overview,” *IEEE Wireless Communications*, vol. 12, no. 2, pp. 19–29, 2005.
- [61] R. E. Ziemer and W. H. Tranter, *Principles of Communication: Systems, Modulation and Noise, 5th Edition*. Wiley, July 2001.